Synthesis and Characterization of Polystyrene/Poly(4-vinylpyridine) Triblock Copolymers by Reversible Addition–Fragmentation Chain Transfer Polymerization and Their Self-Assembled Aggregates in Water

Jian-Jun Yuan,[1] Rui Ma,[1] Qing Gao,[1] Yi-Feng Wang,[1] Shi-Yuan Cheng,[1] Lin-Xian Feng,[2] Zhi-Qiang Fan,[2] Lei Jiang[3]

[1]*College of Chemistry and Materials Sciences, Hubei University, Wuhan 430062, People's Republic of China*
[2]*Institute of Polymer Science, Zhejiang University, Hangzhou 310027, People's Republic of China*
[3]*Institute of Chemistry, Chinese Academy of Sciences, Beijing 100080, People's Republic of China*

Received 25 January 2002; accepted 9 August 2002

ABSTRACT: Reversible addition–fragmentation chain transfer polymerization (RAFT) was developed for the controlled preparation of polystyrene (PS)/poly(4-vinylpyridine) (P4VP) triblock copolymers. First, PS and P4VP homopolymers were prepared using dibenzyl trithiocarbonate as the chain transfer agent (CTA). Then, PS-*b*-P4VP-*b*-PS and P4VP-*b*-PS-*b*-P4VP triblock copolymers were synthesized using as macro-CTA the obtained homopolymers PS and P4VP, respectively. The synthesized polymers had relatively narrower molecular weight distributions ($M_w/M_n < 1.25$), and the polymerization was controlled/living. Furthermore, the polymerization rate appeared to be lower when styrene was polymerized using P4VP as the macro-CTA, compared with polymerizing 4-vinylpyridine using PS as the macro-CTA. This was attributed to the different transfer constants of the P4VP and PS macro-CTAs to the styrene and the 4-vinylpyridine, respectively. The aggregates of the triblock copolymers with different compositions and chain architectures in water also were investigated, and the results are presented. Reducing the P4VP block length and keeping the PS block constant favored the formation of rod aggregates. Moreover, the chain architecture in which the P4VP block was in the middle of the copolymer chain was rather favorable to the rod assembly because of the entropic penalty associated with the looping of the middle-block P4VP to form the aggregate corona and tailing of the end-block PS into the core of the aggregates. © 2003 Wiley Periodicals, Inc. J Appl Polym Sci 89: 1017–1025, 2003

Key words: block copolymers; radical polymerization; poly(4-vinylpyridine); aggregates

INTRODUCTION

The preparation of polymers of predetermined molecular weight, narrow molecular weight distribution, and tailored architecture (e.g., block, graft, and star) has become a major aspect of polymer chemistry in recent years.[1] These well-defined polymers offer a vast range of new and advanced materials for applications in photoelectronics, biomedical materials, and so on. The control on macromolecular structure has been achieved by various methods, such as anionic, cationic, and controlled/living radical polymerization.[1] Controlled/living radical polymerization has several advantages over other living polymerization methods, including tolerance to a wide range of monomers with various functional groups, facile copolymerization, undemanding reaction conditions, and feasibility in the presence of water. The key feature of controlled/living radical polymerization is the dynamic equilibration between the active radicals and various types of dormant species. Currently, three systems have been proved to be most efficient: nitroxide mediated polymerization (NMP),[2] atom transfer radical polymerization (ATRP),[3] and reversible addition–fragmentation chain transfer polymerization (RAFT).[4] NMP carried out in the presence of bulky nitroxide cannot be applied to the polymerization of methacrylates because of fast β-H abstraction. Using ATRP for the polymerization of acidic monomers is limited, and removing catalysts is difficult. In principle, RAFT can be used for any radically polymerizable monomers[5–9] and for preparation of polymers with complex architectures.[5,10–15]

For RAFT, the control of polymerization is achieved by performing it in the presence of a suitable thiocarbonylthio compound that acts as a highly efficient reversible addition–fragmentation chain transfer agent. A simplified mechanism for RAFT, elucidated by Rizzardo,[5] is outlined (Scheme 1) in eq. (1) and the overall process in eq. (2). It involves a reversible chain transfer process in which a thiocarbonylthio agent

Correspondence to: S.-Y. Cheng (scheng@public.wh.hb.cn).

Journal of Applied Polymer Science, Vol. 89, 1017–1025 (2003)

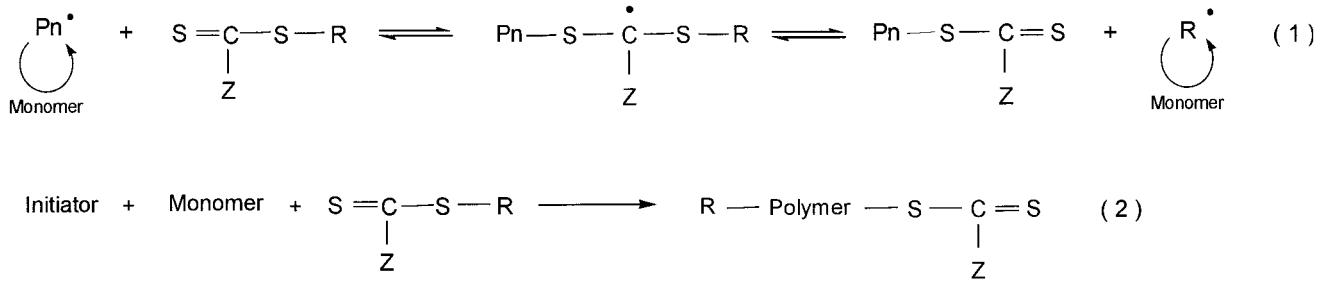

Scheme 1

behaves like a transfer agent, reacting with initiating and propagating radicals to yield a transfer agent and a species able to initiate polymerization. The thiocarbonylthio is transferred between the active and dormant chains, thus maintaining the controlled/living character of polymerization. Recently, additional aspects of the mechanism and kinetics of RAFT have been investigated.[16–18] Moreover, RAFT has been successfully accomplished at ambient temperature by adjusting the structure of thiocarbonylthio[19] and by performing it in emulsion polymerization[20,21] and under ^{60}Co γ-irradiation.[22,23]

Pyridine-containing polymers have attracted interests in recent years because of they can be used in various applications including as water-soluble polymers and coordination reagents for transition metals. Unlike with 2-vinylpyridine,[24] the living polymerization of 4-vinylpyridine has not been well studied until recently,[25–28] despite its more interesting properties resulting from the higher accessibility of the nitrogen atom, that is, easier quarterization to afford polyelectrolytes[29] and hydrogen bonding for constructing hierarchical supermolecular structures.[30] Recently, controlled/living radical polymerization of 4-vinylpyridine has been reported using NMP[31] and ATRP[32] methods. Also, a poly(methyl methacrylate)-*b*-P4VP diblock copolymer with a molecular weight distribution of 1.35 and a molecular weight of 8950 was made by ATRP using poly(methyl methacrylate) as the macroinitiator.[32]

In the present study, polystyrene (PS) and P4VP homopolymers were obtained first, using dibenzyl trithiocarbonate (DBTTC) as the chain transfer agent (CTA). Then, PS-*b*-P4VP-*b*-PS and P4VP-*b*-PS-*b*-P4VP triblock copolymers with various compositions were successfully synthesized using the obtained PS and P4VP homopolymers, respectively, as the macro-CTAs. Moreover, aggregates of the triblock copolymers of different chain architectures and compositions in water were investigated, and the results are presented here.

EXPERIMENTAL

Materials

Styrene and 4-vinylpyridine were stirred over CaH_2 overnight and distilled under reduced pressure prior to use. 2,2′-Azoisobutyronitrile (AIBN) was recrystallized from ethanol. Unless specified, all other reagents were purchased from commercial sources and used without further purification.

Synthesis of DBTTC

The DBTTC was synthesized by reacting CS_2 and 33% aqueous NaOH with benzyl chloride under a phase-transfer catalysis condition (Scheme 2).[33]

Typically, a mixture of 10 mL of CS_2 and 10 mL of 33% aqueous NaOH solution was stirred vigorously at room temperature in a 50-mL round-bottom flask by a magnetic stirrer. The phase transfer catalyst (*n*-Bu_4NHSO_4, 3 mol % to the benzyl chloride used) was then introduced. After stirring for 10 min, 1 mL of benzyl chloride was added. To work up the reaction, the CS_2 layer was first separated, and then the aqueous layer was extracted three times with CS_2 (3×10 mL). The combined CS_2 solution was washed once with water. After being dried over anhydrous Na_2SO_4 and filtered, evaporation of the solvent afforded the DBTTC. The chemical structure was, as elucidated by Fourier transform infrared (FTIR) spectroscopy, (ν, cm^{-1}), 1065 ($\nu_{C=S}$) and, by ^{1}H-NMR (δ, ppm), 2.73 (—CH_2—).

General procedures for synthesis of PS, P4VP, PS-*b*-P4VP-*b*-PS, and P4VP-*b*-PS-*b*-P4VP polymers

The polymerization conditions for various polymers are given in Table I. All polymerizations were carried

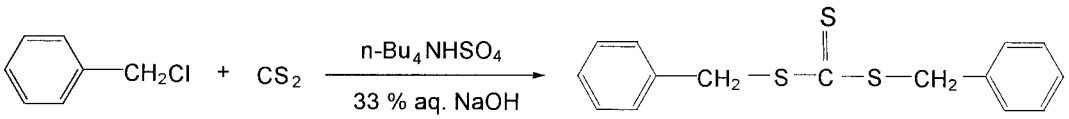

Scheme 2

TABLE I
Polymerization Conditions of Various Polymers by RAFT

Samples	Styrene (mL)	4-Vinylpyridine (mL)	RAFT agents (g)	AIBN (g)	DMF (mL)	Reaction time (h)	Temperature (°C)	Con. (%)
10102	10	—	0.0932[a]	—	—	24	110	67
10182	—	3.5	0.9971[b]	0.0092	1.5	2	80	88
10191	—	3.5	0.9692[b]	0.0084	1.5	2.5	60	86
10261	—	3.5	0.9980[b]	0.0045	1.5	25	60	35
10181	—	7.5	0.0773[a]	0.0200	2.5	7	60	86
10241	3.5	—	0.9933[c]	0.0039	2.5	43	60	32

[a] Dibenzyl trithiocarbonate as RAFT agent; [b] PS (10102) as macro-RAFT agent;
[c] P4VP (10181) as macro-RAFT agent.

out in a 100-mL flask with a rubber septum and a magnetic stir bar. For a certain set of polymerizations, all components were added to the flask under an argon atmosphere and then sufficiently degassed. The sealed flask was immersed in an oil-bath thermostat at a desired temperature. After the reaction time, the polymerization was stopped by cooling. The polymer was precipitated and dried in a vacuum oven. The conversion of the polymerization was determined gravimetrically.

Characterization of polymers

Infrared spectra were recorded on Perkin–Elmer Spectrum One FTIR instruments using KBr tablets. The spectra were obtained over a frequency range of 4000–400 cm^{-1} at a resolution of 4 cm^{-1}. ^{1}H-NMR spectra operated at 300 MHz in the Fourier transform mode were obtained on a Varian XL-300 NMR instrument using $CDCl_3$ as solvent. Molecular weights and molecular weight distributions were determined using gel permeation chromatography (GPC) coupled with multiangle laser-light scattering (MALLS). The system included a Styragel® HMW 6E GPC column (7.8 × 300 mm), a Wyatt OPTILAB RI detector, and a Wyatt multiangle laser-light scattering detector (DAWN E). The MALLS operated at 18 angles, from 26° to 149° and was equipped with a He-Ne laser (690 nm). The column and the RI detector were set at 40°C. The mobile phase was DMF with added Bu_4NBr (0.1 % w/v) at a flow rate of 0.8 mL/min. The polymer solutions of injected sample were filtered through 0.2 μm syringe filters before injection. The molecular weights and polydispersity indexes were measured for the main peaks and were calculated using Wyatt Technology (Astra 473) software. The MALLS detector allowed the calculation of absolute molecular weights.

Preparation of colloid solutions of triblock copolymers

The copolymer solution was prepared by first dissolving the copolymer in DMF and then stirring it overnight at room temperature. To prepare the aggregate solution, the twice-distilled water, a precipitant for the PS block, was added dropwise with stirring into the corresponding copolymer solution, with one drop added every 10–15 s. When the water content reached about 90 wt %, the solution was placed in a dialysis bag and dialyzed against water with a pH of 4 for about 3 days to remove the solvent. Twice-distilled water for dialysis was changed twice a day.

The aggregates were characterized with transmission electron microscopy (TEM) techniques. For TEM measurement a drop of prepared colloid solution was placed on a copper electron microscope (EM) grid. Before sample deposition the EM grid was precoated with a thin film of celloidin. After the drop had been in contact with the grid for a time, excess solution was blotted away using a strip of filter paper. The sample was dried in air for a few hours and then was vacuum-dried. The aggregates were observed on a H-7000 (Hitachi, Japan) transmission electron microscope that was operated at an acceleration of 60 kV.

RESULTS AND DISCUSSION

Polymerization route

First, the PS and P4VP homopolymers were prepared in a controlled manner using DBTTC as the CTA. The trithiocarbonate functionality of both homopolymers was located in the center of the polymer chains (Scheme 3). The middle location of the active function afforded the ability to insert 4-vinylpyridine and styrene monomers at this site, thus forming the PS-*b*-P4VP-*b*-PS and P4VP-*b*-PS-*b*-P4VP triblock copolymers, respectively, in two steps (Scheme 3).

Confirmation of chemical structure of polymers

Figure 1 shows the FTIR spectra of PS, P4VP, PS-*b*-P4VP-*b*-PS, and P4VP-*b*-PS-*b*-P4VP polymers. In contrast to the PS spectra, the strong absorption at 1598 and 1416 cm^{-1}, corresponding to the pyridine ring, and at 821 cm^{-1}, to the single-substituted pyridine ring, appeared in the spectra of PS-*b*-P4VP-*b*-PS. Similarly, in contrast to the P4VP spectra, the adsorption

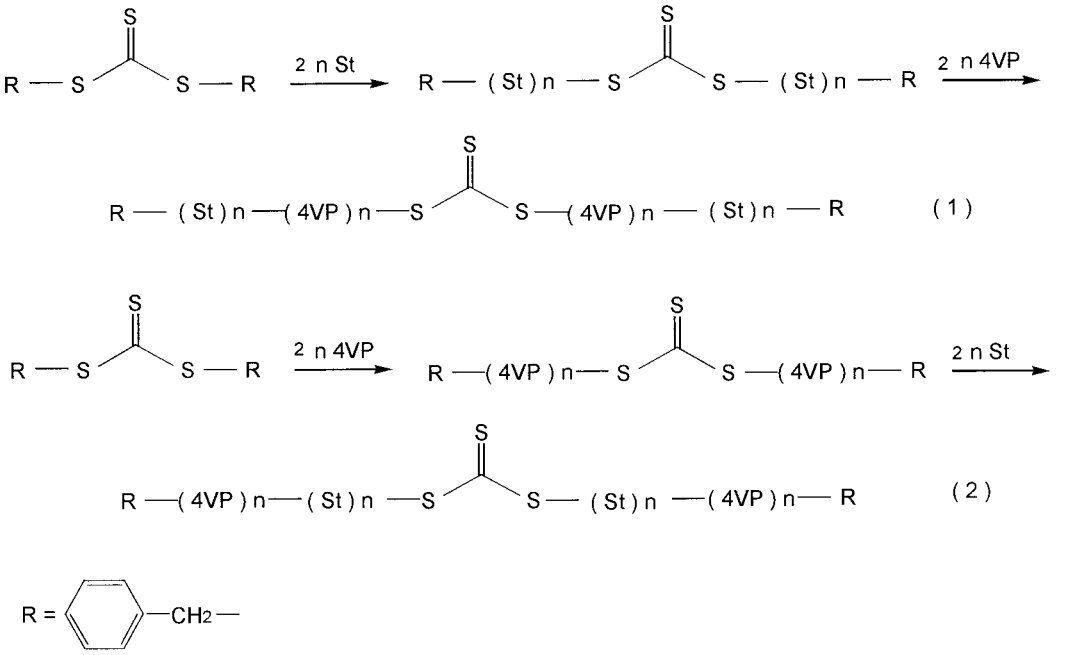

Scheme 3

peaks at 1493 and 1452 cm^{-1}, which were characteristic of the phenyl ring, became stronger, and the peak at 697 cm^{-1}, corresponding to signals of the single-substituted phenyl ring, appeared for the spectra of P4VP-*b*-PS-*b*-P4VP. In addition, all the obtained polymers showed a characteristic IR band of the carbon–sulfur double bond ($\nu_{C=S}$) around 1065 cm^{-1}, which came from the corresponding CTAs.

Figure 2 represents the ^{1}H-NMR spectra of the polymers. Compared with the PS spectra, the PS-*b*-P4VP-*b*-PS spectra showed a peak at $\delta = 8.4$ for two pyridine ring protons. Also, for the spectra of P4VP-*b*-PS-*b*-P4VP, the peak at $\delta = 7.05$ appeared for three of the phenyl ring protons, in contrast to the P4VP spectra. Furthermore, the peak at $\delta = 2.77$, a characteristic signal of the methylene group adjacent to the sulfur atom, remained for all polymers.

Molecular weights, molecular weight distributions, and compositions of the polymers

The molecular weights, molecular weight distributions, and compositions of all polymers are listed in Table II. The compositions of the triblock copolymers were obtained from the integration of the peaks associated with the protons of the phenyl and pyridine rings. Clearly, the final observed polydispersity index (M_w/M_n) of less than 1.24 was well below the theoretical lowest limit of 1.50 for a conventional free-radical polymerization and could be considered a narrower distribution. The refractive index (RI) traces for the PS macro-CTA and the corresponding triblock copolymers are shown in Figure 3, and the P4VP macro-CTA and relative block copolymer are illustrated in Figure 4. Obviously, all curves had a single peak without a marked shoulder. From combining the shape of the

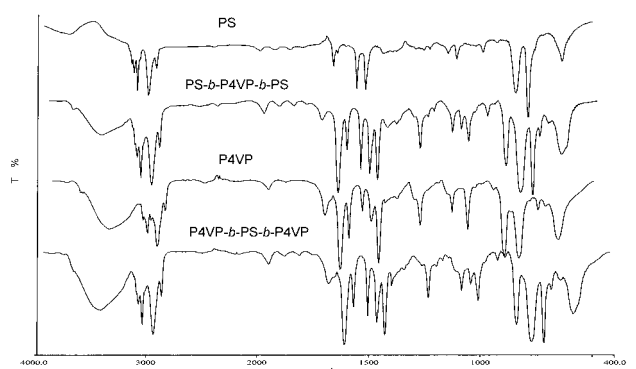

Figure 1 FTIR spectra of PS, P4VP, PS-*b*-P4VP-*b*-PS, and P4VP-*b*-PS-*b*-P4VP polymers.

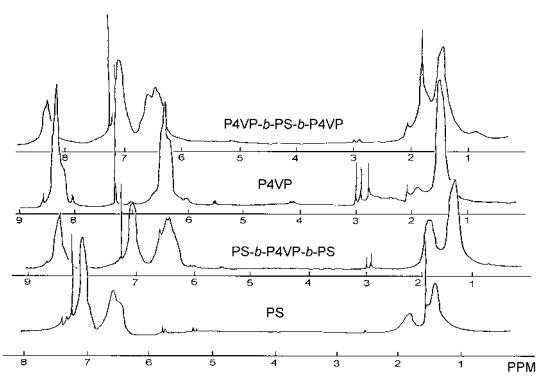

Figure 2 ^{1}H-NMR spectra of PS, P4VP, PS-*b*-P4VP-*b*-PS, and P4VP-*b*-PS-*b*-P4VP polymers.

TABLE II
Molecular Weights, Molecular Weight Distributions, and Compositions of Various Polymers by RAFT

Samples	Polymers	M_n[a]	M_w/M_n	PS contents (weight %)[b]
10102	PS	12110	1.16	100
10182	PS-*b*-P4VP-*b*-PS	6055-11690-6055	1.11	38.3
10191	PS-*b*-P4VP-*b*-PS	6055-14910-6055	1.09	27.7
10261	PS-*b*-P4VP-*b*-PS	6055-5880-6055	1.15	44.0
10181	P4VP	16290	1.14	0
10241	P4VP-*b*-PS-*b*-P4VP	8145-13690-8145	1.24	55.7

[a] Molecular weights determined from GPC–MALLS;
[b] PS contents were obtained from ^{1}H-NMR.

GPC curves and the narrower molecular weight distributions, it appears that there was no significant homopolymer impurities in the block copolymers. Therefore, most of the chain centers of both the PS and P4VP macro-CTAs were functionalized with trithioester groups and underwent a subsequent addition with the corresponding comonomers. Finally, the combination of RAFT background and various confirmation from IR, ^{1}H-NMR, and GPC indicated that the polymers obtained were well defined and the polymerization was controlled/living.

In addition, the experimental results revealed that the polymerization behavior of extending the polymers was different when using PS as the macro-CTA for the synthesis of PS-*b*-P4VP-*b*-PS triblock copolymer than when using P4VP for P4VP-*b*-PS-*b*-PS synthesis. It was found that the conversion reached 35% after 25 h for making PS-*b*-P4VP-*b*-PS using PS as the macro-CTA; meanwhile, about 43 h was needed to reach 32% conversion for extending P4VP into the P4VP-*b*-PS-*b*-P4VP triblock copolymer (as shown in Table I). At the same time, it was worthy to note that the molecular weight distribution of the P4VP-*b*-PS-*b*-P4VP triblock copolymer reached up to 1.24. In contrast, all PS-*b*-P4VP-*b*-PS triblock copolymers had a polydispersity less than 1.16. The difference in polymerization behavior probably resulted from the difference in the transfer constants between PS and P4VP macro-CTAs to the 4-vinylpyridine and styrene monomers, respectively. Generally, one requirement for forming a narrow polydispersity block copolymer was that the first-formed macro-CTA (A block) should have a high transfer constant in the subsequent polymerization step in order to give another block (B block). This required that the leaving group ability of propagating radical A · was comparable to or greater than that of the propagating radical B · under reaction conditions.[13] In our polymerization system, when A was a P4VP chain, the transfer constants of P4VP-S-C(S)-S-P4VP in the styrene polymerization appeared to be lower. This was attributed to the P4VP-propagating radicals being poor, leaving groups with a PS-propagating radical and causing adduct radical (A) to partition strongly in favor of starting materials

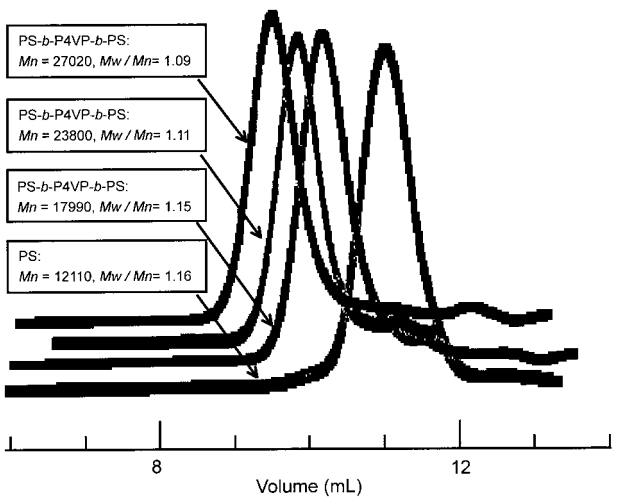

Figure 3 GPC traces of PS macro-CTA and corresponding PS-*b*-P4VP-*b*-PS triblock copolymer.

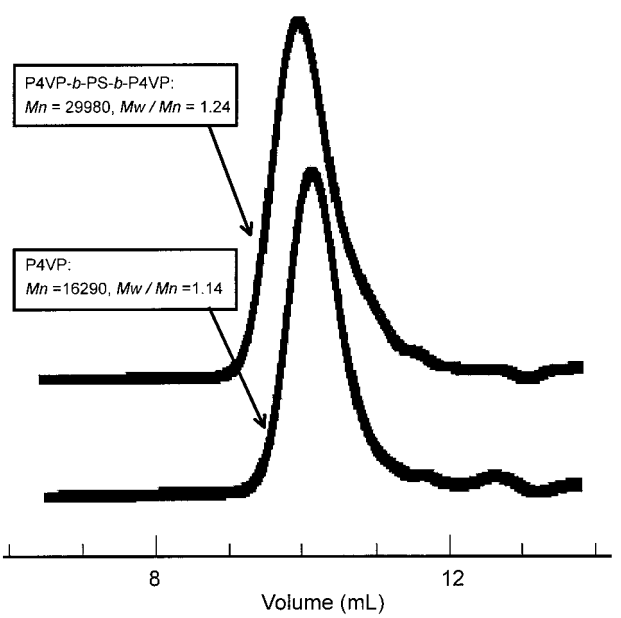

Figure 4 GPC traces of P4VP macro-CTA and corresponding P4VP-*b*-PS-*b*-P4VP triblock copolymer.

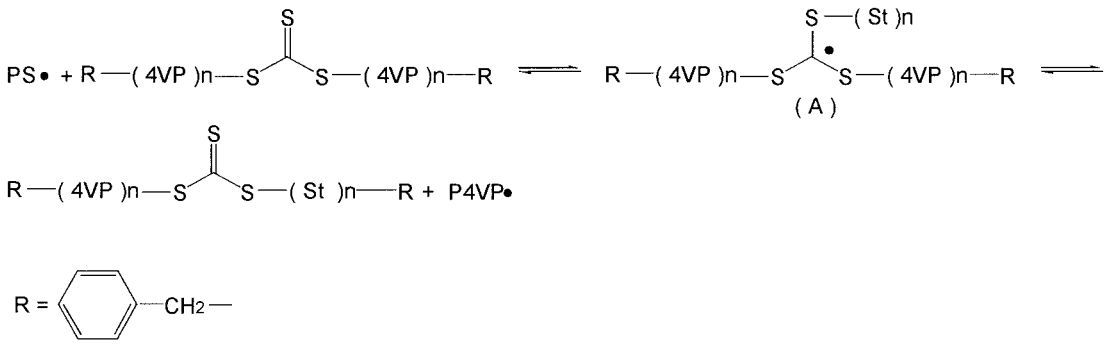

Scheme 4

(Scheme 4). As a result, slower polymerization occurred for synthesis of P4VP-*b*-PS-*b*-P4VP from P4VP macro-CTA than for that of the PS-*b*-P4VP-*b*-PS triblock copolymers. Moreover, relatively higher polydispersity was found for P4VP-*b*-PS-*b*-P4VP triblock copolymers.

Mechanism

The mechanism by which RAFT polymerization is carried out in the presence of DBTTC could be as follows (Scheme 5), which includes initiation, chain transfer, chain equilibrium, and termination. In the early stages of polymerization, the DBTTC was rapidly transferred into a macro-CTA by reaction with a propagating radical (Pn·). At the same time, this macro-CTA could also have reacted with another propagating radical and been transferred into a macro-CTA with trithiocarbonate in the center of the chain. The liberated radical (R ·) reacted with a monomer to form a new propagation radical (Pn ·). Once the DBTTC was consumed, chain equilibrium was established between the active and dormant species, providing polymerization with a controlled/living character. In RAFT the chain equilibrium could minimize termination by creating a steady, low concentration of short-lived, active radical chain ends.

Aggregates of triblock copolymers in water

Self-assembled aggregates with various morphologies can be formed on the dissolving of the block copolymers into the selective solvents. Recently, the Eisenberg group[34] reported on the aggregation behavior of P4VP-*b*-PS diblock copolymers in water. In fact, the self-assembly behavior of block copolymers strongly depends on the chain architecture.[35] Clearly, the aggregation behavior of block copolymers based on different chain architectures is very interest. Here we were concerned with the aggregates of P4VP/PS triblock copolymers with different architectures and compositions. Three samples were used: 10182, 10261, and 10241. The 10182 and 10261 samples have the same chain architecture, with P4VP in the center of the copolymer chain and the same end-block PS length, but a different middle-block P4VP length. The 10182 has longer P4VP chain than the 10261. In contrast, the 10241 has a inverse chain architecture with the PS block in the center of the copolymer chain and the P4VP blocks at the end of the chain.

Conventionally, self-assembled aggregates of block copolymers with a relative longer soluble middle-block A are frequently prepared by directly dissolving the copolymers into the solvent selective for the A block. In contrast, it was difficult for the triblock copolymers investigated in present work to self-assemble in water by directly dissolving the copolymer into pure water because of the relatively bulkier PS blocks. So, an alternative method was used: first, dissolving the copolymer into the DMF; then adding water to the copolymer solutions with stirring in order to induce the self-assembly of copolymer. DMF was a good solvent for both blocks, whereas water was a good solvent only for the block P4VP but was a precipitant for the block PS. During water addition to the initial copolymer solutions, the quality of the solvent for the block PS gradually decreased. For the P4VP-*b*-PS-*b*-P4VP block copolymers, aggregation involved looping of the hydrophobic PS middle block into the core of the aggregates and tailing two hydrophilic P4VP end blocks to form the corona of aggregates [as shown in Fig. 5(A)]. In contrast, for the PS-*b*-P4VP-*b*-PS copolymers, aggregation involved looping of middle-block P4VP and tailing of end-block PS [as shown in Fig. 5(B)]. In the early stage of aggregation of the triblock copolymers, the relatively low water content in the system allowed the exchange of the copolymer chains between the unimers and aggregates to proceed at a significant rate. Thus, a thermodynamic equilibrium could be operative for aggregation. As more water was added and more common solvent was extracted from the core of aggregates, the rate of copolymer chain exchange became low because of the decreased solubility of the copolymers. As a result, the aggre-

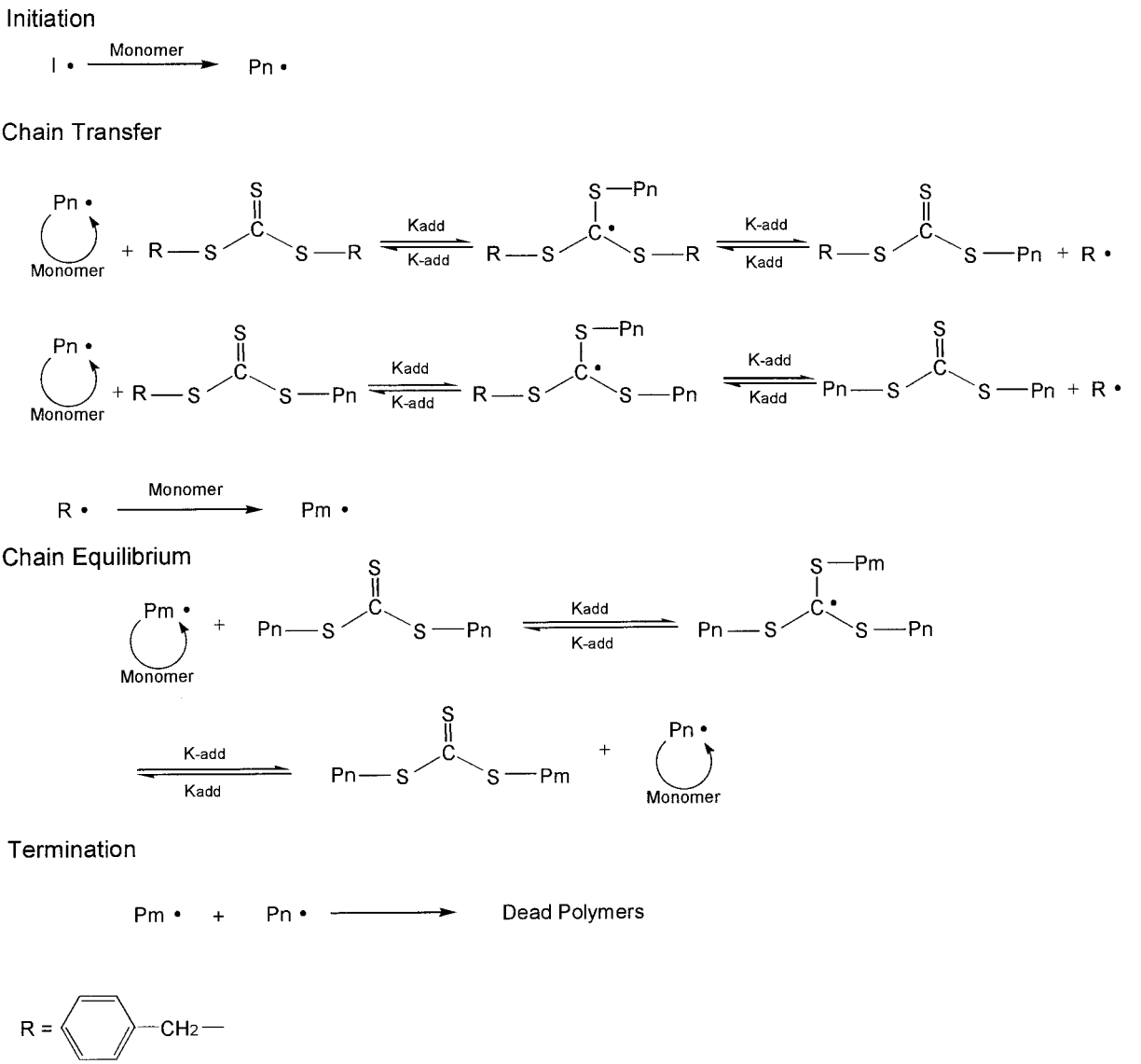

Scheme 5

gates became kinetically frozen with any further addition of water.

Composition

Figure 6(A,B) shows the TEM photographs of the self-assembled aggregates in water of, respectively, 10182 and 10261. The aggregates were made from a 1 wt % triblock copolymer solution in DMF. Clearly, for 10182 the majority of aggregates had pearl-necklace and short rod and short-branched rod morphologies; discrete spheres also were observed. In contrast, 10261 showed an increasing ability to form rods: straight rods of various lengths predominated, and spheres were observed only occasionally. The rod-forming behavior of 10261 can be attributed to the decrease of the P4VP length at a given PS length.

Generally, the morphology of block copolymer aggregates depends on the balance between three of the major forces acting on the system. These include the stretching of the core-forming blocks, the intercoronal interactions, and the interfacial energy between the solvent and the micellar core.[36] The two triblock copolymers investigated here have a constant PS block length but different P4VP block lengths. With decreasing P4VP block length, the repulsive interactions between the coronal block chains decreased; thus, more chains aggregated, leading to larger aggregates. However, the PS chains must reach from the center of the core to the core–coronal interface, and in general, the larger the PS core, the greater is the average core–chain stretching. When the aggregates became larger, the entropic penalty of the core–chain stretching afforded simple spheres unfavorable as a low-energy

morphology, and rods formed with a decreased core diameter. Therefore, reducing the P4VP block and keeping the PS block constant rendered the sphere–rod transition.

Chain architecture

Figure 7 shows the TEM photograph of self-assembled aggregates of 10241 in water. The aggregates were made from a 1 wt % copolymer solution in DMF. Clearly, most aggregates appeared to be discrete spheres, with some pearl-necklace and short rod and short-branched rod aggregates. In contrast to the aggregates of 10182 and 10261, more discrete spheres were observed. In other words, the 10182 and 10261 aggregates had an increasing ability to assemble into a rod morphology in comparison with 10241. Generally, a higher content of insoluble blocks was more favorable to rod formation than to sphere formation.[34] Therefore, given its composition, 10241 should have a higher tendency to rod formation than should 10182 and 10261 because the 10241 (PS, 55.7 wt %) had a higher content of the PS block relative to 10182 (PS, 38.3 wt %) and 10261 (PS, 44.0 wt %). Clearly, this deduction was contradictive to the experimental results obtained.

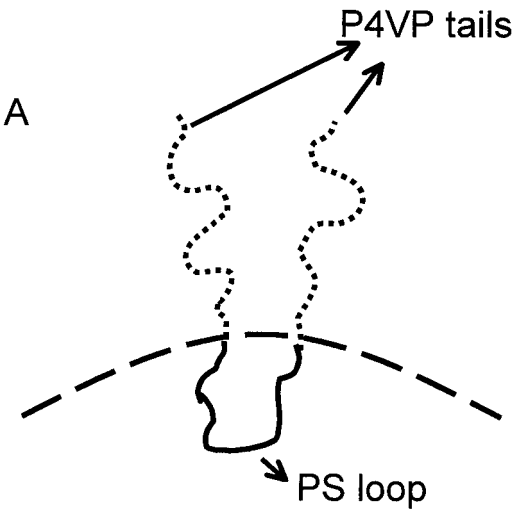

Figure 5 Schemes of chain conformation in aggregates in water of (A) P4VP-*b*-PS-*b*-P4VP triblock copolymer and (B) PS-*b*-P4VP-*b*-PS triblock copolymer.

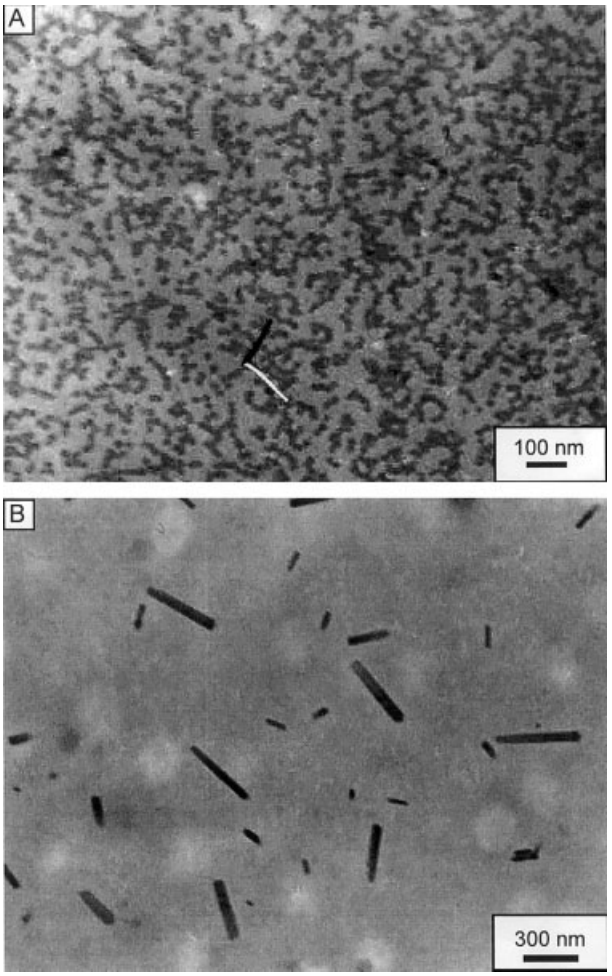

Figure 6 TEM photographs of self-assembled aggregates of (A) 10182 and (B) 10261 in water. The aggregates were made from a 1 wt % triblock copolymer solution in DMF.

The difference in chain architecture between the two copolymers strongly contributed to the higher ability for rod formation in 10182 and 10261 than in 10241. In contrast, the looping in aqueous media of P4VP middle block and tailing into aggregate core of the PS end blocks of 10182 and 10261 were associated with a greater penalty of entropy, thus resulting in a decreasing ability for copolymer aggregation.[36] At the same time, the assembly of rods could accommodate reducing aggregation ability better than could sphere aggregates because of the decreased curvature of rod morphology compared with sphere morphology. The increase of rod formation

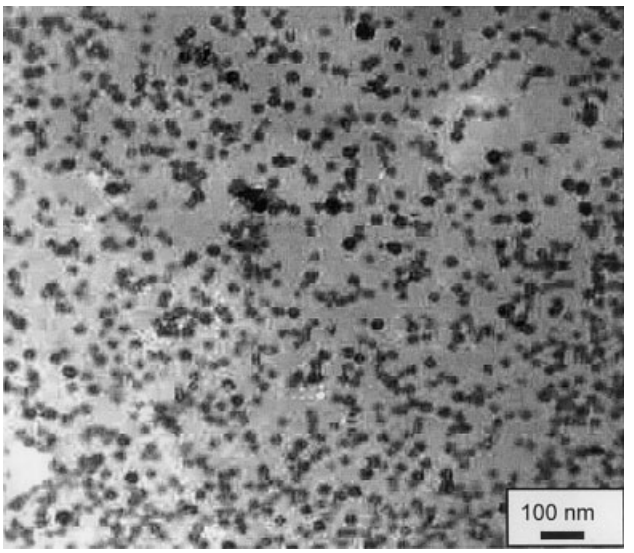

Figure 7 TEM photographs of P4VP-*b*-PS-*b*-P4VP triblock copolymer aggregates formed in water. The aggregates were made from a 1 wt % triblock copolymer solution in DMF.

ability gained for 10182 and 10261 from chain architecture surpassed that for 10241 from its composition. As a result, the overall effect was that 10182 showed a higher ability for rod aggregation and 10261 than 10241 did.

CONCLUSIONS

The well-defined PS, P4VP, PS-*b*-P4VP-*b*-PS, and P4VP-*b*-PS-*b*-P4VP polymers were controllably synthesized by RAFT. All polymers had relatively narrower molecular weight distributions ($M_w/M_n < 1.25$), and the polymerization proved to be controlled/living. Moreover, the polymerization rate appeared to be relatively lower for the polymerization of styrene using P4VP as macro-CTA to form P4VP-*b*-PS-*b*-P4VP compared with the polymerization of 4-vinylpyridine using PS as macro-CTA to form PS-*b*-P4VP-*b*-PS. This was a result of the lower transfer constants of the P4VP macro-CTA to styrene compared with those of PS macro-CTA to 4-vinylpyridine.

The morphologies of the self-assembled aggregates strongly depended on composition and chain architecture. Reducing the P4VP block length and keeping the PS block constant was proved to favor the formation of rod aggregates. Moreover, a chain architecture with the P4VP block in the middle of the triblock copolymer chain was strongly favorable to rod assembly because of the entropic penalty associated with the looping of the middle-block P4VP to form the aggregate corona and the tailing of end-block PS into the core of the aggregates.

References

1. Matyjaszewski, K. Macromol Symp 2001, 174, 51.
2. Georges, M. K.; Veregin, R. P. N.; Kazmaier, P. M.; Hamer, G. K. Macromolecules 1993, 26, 2987.
3. Wang, J. S.; Matyjaszewski, K. J Am Chem Soc 1995, 117, 5614; Kato, M.; Kamigaito, M.; Sawamoto, M.; Higashimura, T. Macromolecules 1995, 28, 1721.
4. Chiefari, J.; Chong, Y. K.; Ercole, F.; Krstina, J.; Jeffery, J.; Le, T. P. T.; Mayadunne, R. T. A.; Meijs, G. F.; Moad, C. L.; Moad, G.; Rizzardo, E.; Thang, S. H. Macromolecules 1998, 31, 5559.
5. Rizzardo, E.; Chiefari, J.; Mayadunne, R.; Moad, G.; Thang, S. Macromol Symp 2001, 174, 209.
6. Sumerlin, B. S.; Donovan, M. S.; Mitsukami, Y.; Lowe, A. B.; McCormick, C. L. Macromolecules 2001, 34, 6561.
7. Kanagasabapathy, S.; Sudalai, A.; Benicewicz, B. C. Macromol Rapid Commun 2001, 22, 1076.
8. Ladaviere, C.; Dorr, N.; Claverie, J. P. Macromolecules 2001, 34, 5370.
9. Mitsukami, Y.; Donovan, M. S.; Lowe, A. B.; McCormick, C. L. Macromolecules 2001, 34, 2248.
10. Stenzel-Rosenbaum, M.; Davis, T. P.; Chen, V.; Fane, A. G. J Polym Sci, Part A: Polym Chem 2001, 39, 2777.
11. Zhuang, R. C.; Chen, H. H.; Lin, J.; Ye, J. L.; Zou, Y. S. Acta Polymerica Sinica 2001, 3, 288.
12. Zhu, M. Q.; Wei, L. H.; Li, M.; Jiang, L.; Du, F. S.; Li, Z. C.; Li, F. M. Chem Commun 2001, 365.
13. Chong, Y. K.; Le, T. P. T.; Moad, G.; Rizzardo, E.; Thang, S. H. Macromolecules 1999, 32, 2071.
14. Mayadunne, R. T. A.; Rizzardo, E.; Chiefari, J.; Kristina, J.; Moad, G.; Postma, A.; Thang, S. H. Macromolecules 2000, 33, 243.
15. Shinoda, K.; Matyjaszewski, K. Macromol Rapid Commun 2001, 22, 1176.
16. Goto, A.; Sato, K.; Tsujii, Y.; Fukuda, T.; Moad, G.; Rizzardo, E.; Thang, S. H. Macromolecules 2001, 34, 402.
17. Monteiro, M. J.; de Brouwer, H. Macromolecules 2001, 34, 349.
18. Barner-Kowollik, C.; Quinn, J. F.; Nguyen, T. L. U.; Heuts, J. P. A.; Davis, T. P. Macromolecules 2001, 34, 7849; Barner-Kowollik, C.; Quinn, J. F.; Morsley, D. R.; Davis, T. P. J Polym Sci, Part A: Polym Chem 2001, 39, 1353.
19. Quinn, J. F.; Rizzardo, E.; Davis, T. P. Chem Commun 2001, 1044.
20. Tsavalas, J. G.; Schork, F. J.; de Brouwer, H.; Monteiro, M. J. Macromolecules 2001, 34, 3938; Monteiro, M. J.; de Barbeyrac, J. Macromolecules 2001, 34, 4416.
21. Butte, A.; Storti, G.; Morbidelli, M. Macromolecules 2001, 34, 5885.
22. Bai, R. K.; You, Y. Z.; Pan, C. Y. Macromol Rapid Commun 2001, 22, 315.
23. Bai, R. K.; You, Y. Z.; Zhong, P.; Pan, C. Y. Macromol Chem Phys 2001, 202, 1970.
24. Lee, C. L.; Smid, J.; Szwarc, M. Trans Faraday Soc 1963, 59, 1192; Tardi, M.; Sigwalt, P. Eur Polym J 1973, 9, 1369.
25. Varshney, S. K.; Zhong, X. F.; Eisenberg, A. Macromolecules 1993, 26, 701
26. Nugay, N.; Kucukyavuz, Z.; Kucukyavuz, S. Polym Int 1993, 32, 93
27. Creutz, S.; Teyssie, P.; Jerome, R. Macromolecules 1997, 30, 1.
28. Creutz, S.; Teyssie, P.; Jerome, R. Macromolecules 1997, 30, 5596.
29. Frere, Y.; Gramain, P. Macromolecules 1992, 25, 3184.
30. Ruokolainen, J.; ten Brinke, G.; Ikkala, O. Adv Mater 1999, 11, 777.
31. Fischer, A.; Brembilla, A.; Lochon, P. Macromolecules 1999, 32, 6069.
32. Xia, J.; Zhang, X.; Matyjaszewski, K. Macromolecules 1999, 32, 3531.
33. Lee, A. W. M.; Chan, W. H.; Wong, H. C. Syn Commun 1988, 18, 1531.
34. Shen, H.; Zhang, L.; Eisenberg, A. J Am Chem Soc 1999, 121, 2728.
35. Booth, C.; Attwood, D. Macromol Rapid Commun 2000, 21, 501.
36. Zhang, L.; Eisenberg, A. J Am Chem Soc 1999, 118, 3168.